Biochemistry

© Copyright 1983 by the American Chemical Society Volume 22, Number 8 April 12, 1983

*Articles*

# Rotational Freedom of Tryptophan Residues in Proteins and Peptides†

Joseph R. Lakowicz,* Badri P. Maliwal, Henryk Cherek, and Aleksander Balter

ABSTRACT: We studied the rotational motions of tryptophan residues in proteins and peptides by measurement of steady-state fluorescence anisotropies under conditions of oxygen quenching. By fluorescence quenching we can shorten the fluorescence lifetime and thereby decrease the average time for rotational diffusion prior to fluorescence emission. This method allowed measurement of rotational correlation times ranging from 0.03 to 50 ns, when the unquenched fluorecence lifetimes are near 4 ns. A wide range of proteins and peptides were investigated with molecular weights ranging from 200 to 80 000. Many of the chosen substances possessed a single tryptophan residue to minimize the uncertainties arising from a heterogeneous population of fluorophores. In addition, we also studied a number of multi-tryptophan proteins. Proteins were studied at various temperatures, under conditions of self-association, and in the presence of denaturants. A wide variety of rotational correlation times were found. As examples we note that the single tryptophan residue of myelin basic protein was highly mobile relative to overall protein rotation whereas tryptophan residues in human serum albumin, RNase $T_1$, aldolase, and horse liver alcohol dehydrogenase were found to be immobile relative to the protein matrix. These results indicate that one cannot generalize about the extent of segmental mobility of the tryptophan residues in proteins. This physical property of proteins is highly variable between proteins and probably between different regions of the same protein.

The dynamic properties of proteins are of interest for understanding the physical properties of these macromolecules and because of the possible significance of structural fluctuations in catalysis (Carreri, 1974; Carreri et al., 1979). A variety of physical methods have been utilized for quantifying protein dynamics (Gurd & Rothgeb, 1979; Karplus & McCammon, 1981). These include fluorescence spectroscopy, X-ray diffraction, solvent exchange, magnetic resonance, and molecular dynamics calculations. To date, conformational freedom has been detected in a variety of conditions and under a variety of circumstances. The detected motions range from the conformational freedom of large regions of the proteins to the smaller motions of the side chains of individual amino acid residues. As examples we note the following: The rapid rates of hydrogen exchange in proteins revealed solvent penetration into the interior of many proteins or partial unfolding of the proteins (Hilton & Woodward, 1978; Wagner & Wuthrich, 1978; Englander, 1975). Independent rotational displacements of the $F_{ab}$ portions of immunoglobulins were detected by both steady-state and time-resolved fluorescence anisotropies (Hanson et al., 1981; Liv et al., 1981; Wahl & Weber, 1967; Nezlin et al., 1970; Yguerabide et al., 1970). The general flexibility of proteins on the nanosecond time scale was initially revealed by measurements of oxygen quenching of tryptophan fluorescence (Lakowicz & Weber, 1973a,b), and a similar but less pronounced flexibility in some but not all proteins was found by acrylamide and iodide quenching (Eftink & Ghiron, 1976, 1977; Bushueva et al., 1980). On a more specific level the rotational freedom of individual tryptophan residues in proteins was detected by time-resolved and lifetime-resolved fluorescence anisotropies (Munro et al., 1979; Lakowicz & Weber, 1980; Ross et al., 1981a). Magnetic resonance methods have also revealed rapid rotational motions of aromatic and aliphatic side chains of amino acids (Gurd & Rothgeb, 1979). And finally, molecular dynamics calculations (McCammon et al., 1977) have indicated significant displacements of amino acid residues of proteins on the picosecond time scale. These motions may be a result of inherent thermodynamic fluctuations of the small protein molecules (Copper, 1976).

In this paper we describe the use of fluorescence methods to further investigate the rotational freedom of tryptophan residues in proteins and peptides. Fluorescence spectroscopic methods are suitable because of the high sensitivity of this technique and its natural time window on the nanosecond time

† From the Department of Biological Chemistry, University of Maryland School of Medicine, Baltimore, Maryland 21201. *Received August 3, 1982.* This work was supported by Grant PCM 80-41320. This work was done during the tenure of an Established Investigatorship (to J.R.L.) from the American Heart Association (78-151). A.B. and H.C. were on leave from the Institute of Physics, Nicholas Copernicus University, Torun, Poland.

0006-2960/83/0422-1741$01.50/0 © 1983 American Chemical Society

Scheme I

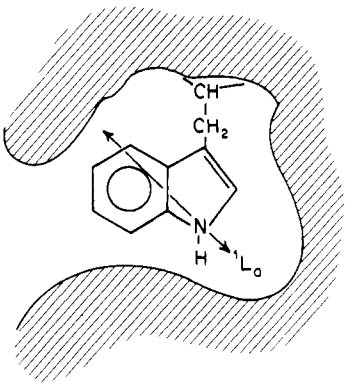


scale. We quantified the rotational displacement of tryptophan residues by lifetime-resolved measurements of fluorescence anisotropy. Measurements of fluorescence anisotropy reveal the average angular displacement of the fluorophore during the lifetime of the excited state. This duration can be decreased by oxygen quenching, allowing less time for angular displacement and thus higher steady-state anisotropies (Lakowicz, 1980). This procedure was used previously for membrane-bound fluorophores (Lakowicz et al., 1979; Lakowicz & Knutson, 1980) and for proteins containing several tryptophan residues (Lakowicz & Weber, 1980). Previously we demonstrated that the oxygen concentrations and pressures required for quenching did not perturb protein structure or enzymatic activity (Lakowicz & Weber, 1973b). Hence, this procedure provides a reliable measure of the motional freedom of tryptophan residues. Lifetime-resolved anisotropies have been obtained with quenchers other than oxygen (Teale & Badley, 1970; Chen, 1973; Bentz et al., 1975).

The primary barriers to rotational displacement of the indole ring are probably the surrounding protein matrix and hydrogen bonding with polar regions of this matrix. At our chosen optical conditions the emission dipole lies approximately along the long axis of the indole ring (Kawski & Sepiol, 1972; Konev, 1967). Displacement of the electric vector requires rotation of the indole ring around its methylene linkage to the peptide backbone (Scheme I). We expect that the displacements of the indole residue will be representative of the time scale and amplitude of the motions of the surrounding protein matrix. This assumption that mobility of the tryptophan residues requires complementary mobility of the protein matrix is supported by the studies of Richards (1974, 1977), who found that the amino acid residues in proteins are packed as closely as small organic molecules in crystals.

We examined a number of peptides and proteins. Some contained only a single tryptophan residue. These included several tripeptides, gastrin, cosyntropin, glucagon, melittin, monellin, myelin basic protein, RNase $T_1$,[1] micrococcal nuclease, human serum albumin, and chorionic gonadotropin. The effects of the salt-induced self-association of melittin was studied, as were the effects of denaturation on the tryptophan correlation times of HSA and monellin. Horse liver alcohol dehydrogenase, which contains two tryptophan residues per subunit (Trp-15 and Trp-314), one of which is buried, was studied because of the dispute about the accessibility of the internal residue (Trp-314) to oxygen quenching of its phosphorescence (Saviotti & Galley, 1974; Vanderkooi et al., 1982; Eftink & Jameson, 1982). In addition, we studied a number of proteins which contain more than a single tryptophan residue. For multi-tryptophan proteins a detailed interpretation of the results is hindered by the heterogeneity of the fluorescence emission. Nonetheless, these data enhance our general understanding of the dynamics of tryptophan residues in proteins.

[1] Abbreviations: NATA, *N*-acetyl-L-tryptophanamide; HSA, human serum albumin; LADH, horse liver alcohol dehydrogenase; MBP, myelin basic protein; Gdn·HCl, guanidine hydrochloride; apo-Hb, apohemoglobin; RNase $T_1$, ribonuclease $T_1$.

## Theory

*Segmental Motions of a Protein-Bound Fluorophore.* The rotational displacement of a tryptophan residue is a superimposition of the overall rotational motion of the protein and the motion of the residue within the protein matrix. A number of theoretical treatments of this subject exist (Wallach, 1967; Lipari & Szabo, 1980; Kinosita et al., 1977; Gottlieb & Wahl, 1963). These treatments lead to various expressions for the time-dependent decay of the emission anisotropy $r(t)$. For instance, for a completely asymmetric body, the time-resolved anisotropy is expected to be a sum of five exponentials (Belford et al., 1972). In practice, only two exponential terms are expected to be experimentally observable. Furthermore, for NATA in viscous solvents, only a single decay constant has been observed (Munro et al., 1979; Ross et al., 1981a). For this reason the decays of anisotropy are well approximated by the expressions we describe below. In the absence of rotational diffusion the anisotropy is $r_0$. The anisotropy, $r(t)$, ultimately decays to zero because of either rotation of the tryptophan residues within the protein matrix or overall rotation of the protein. Depending upon the freedom of the residue within the protein matrix some fraction ($\alpha$) of the total anisotropy ($r_0$) is lost due to the segmental motion. The remaining anisotropy, $r_0(1 - \alpha)$, decays as a result of rotational diffusion of the protein. For independent segmental and rotational motions the anisotropy is given by the product of these separate factors. Hence

$$r(t) = r_0[\alpha e^{-t/\phi_T} + (1 - \alpha)]e^{-t/\phi_P} \quad (1)$$

where $\phi_T$ is the correlation time for motion of the residue within the protein matrix and $\phi_P$ the correlation time for overall protein rotation. This latter value may be estimated by using

$$\phi_P = f\frac{\eta V}{kT} \quad (2)$$

where $V$ is the volume of the protein, $\eta$ is the viscosity, and $f$ is a factor depending on the shape and hydration of the protein. For globular proteins the calculated values of $\phi_P$ agree well with the observed values when $f = 2$, as may be judged by comparison with measured correlation times (Yguerabide et al., 1970; Massey & Churchich, 1979; Bauer et al., 1975).

We have not directly measured the time-resolved decays of anisotropy. Rather, steady-state anisotropies were measured as the fluorescence lifetime was decreased by oxygen quenching. These lifetimes were calculated from

$$\tau = \frac{\tau_0}{1 + K[O_2]} \quad (3)$$

where $\tau_0$ and $\tau$ are the lifetimes in the absence and presence of quencher and $K$ is the collisional Stern–Volmer quenching constant. The validity of eq 3 for oxygen quenching of protein fluorescence was previously demonstrated (Lakowicz & Weber, 1973a,b). The steady-state anisotropies at various lifetimes [$r(\tau)$] are given by the average of $r(t)$ over the total decay of fluorescence intensity:

$$r(\tau) = \frac{\int_0^\infty r(t)e^{-t/\tau}\,dt}{\int_0^\infty e^{-t/\tau}\,dt} \quad (4)$$

Application of eq 4 to eq 1 yields

$$r(\tau) = \frac{\alpha r_0}{1 + \left(\frac{1}{\phi_T} + \frac{1}{\phi_P}\right)\tau} + \frac{(1-\alpha)r_0}{1 + \frac{\tau}{\phi_P}} \quad (5)$$

When the internal motion is more rapid than overall protein rotation, that is, $\phi_T \ll \phi_P$, eq 5 simplifies to

$$r(\tau) = \frac{\alpha r_0}{1 + \tau/\phi_T} + \frac{r_0(1-\alpha)}{1 + \tau/\phi_P} \quad (6)$$

Then, the internal motion results in a rapid loss of part of the initial anisotropy ($\alpha r_0$). The remainder [$r_0(1 - \alpha)$] decays by overall rotational diffusion of the protein.

From eq 5 and 6 we can predict the effects of $\phi_P$ and $\phi_T$ on the lifetime-resolved anisotropies. The relative importance of each motion is determined by the amplitude $\alpha$ and by the ratio $\tau/\phi_T$ and $\tau/\phi_P$. If $\alpha = 0$, the residue is immobile relative to the protein matrix, and the anisotropy is determined by the value of $\phi_P$. If the residue is completely free to rotate, independently of the protein, then $\alpha = 1$ and the anisotropy would be determined by $\phi_T$. Now suppose $\alpha$ is nonzero but less than one, and suppose the overall rotational correlation time is much larger than the fluorescence lifetime $\phi_P \gg \tau$. Then, rotation of the entire protein does not result in any loss of anisotropy, and the values for $r(\tau)$ are determined by the time scale of the internal motion ($\phi_T$) and by amplitude of this motion ($\alpha$). Consider the effect of an internal motion which is more rapid then the shortest quenched lifetime, $\phi_T \ll \tau$. The effect of this internal motion (eq 6) is complete prior to emission, and the overall rotation of the protein determines the decay of the residual anisotropy, $r_0(1 - \alpha)$. The existence of the internal motion can be judged from the value of the anisotropy at $\tau = 0$, which will be designated by $r(0)$. Generally, we expect $r(0)$ to coincide with $r_0$ because both should represent a spectral property of the fluorophore, this being the anisotropy which is unaffected by rotational diffusion. In our case, and in many experimental situations, $r(0)$ and $r_0$ are not equal, generally because of the presence of motions too rapid to be resolved with existing instrumentation and methodology.

In general, one can relate the anisotropy to the angular displacement ($\theta$) of the fluorophore according to

$$\frac{r}{r_0} = \frac{3\langle\cos^2\theta\rangle - 1}{2} \quad (7)$$

Brackets denote the average over the ensemble of fluorophores. We note that $\theta$ is not the actual angle for motion of any given fluorophore. However, it is convenient to consider the angular freedom of fluorophores in terms of the calculated values of $\theta$. A value of 0° corresponds to no rotational freedom, and an angle of 54.7° corresponds to complete depolarization. For a protein-bound tryptophan residue the apparent value of the anisotropy at $t = 0$ reveals the average angular displacement of the residue ($\theta_T$) which is too rapid to be revealed by the experiment:

$$\frac{r(0)}{r_0} = \frac{3\langle\cos^2\theta_T\rangle - 1}{2} = 1 - \alpha \quad (8)$$

This expression relating $r(0)$ and $r_0$ to the degree of flexibility is equivalent to that described previously by Weber (1952).

For completeness we note that time-resolved anisotropies are frequently fit to an equation of the form

$$r(t) = r_0\sum_i \alpha_i e^{-t/\phi_i} \quad (9)$$

In the lifetime domain eq 9 becomes

$$r(\tau) = r_0\sum_i \frac{\alpha_i}{1 + \tau/\phi_i} \quad (10)$$

The shorter correlation time is generally equated with the segmental motion, but one should recall that this shorter value of $\phi_i$ contains both $\phi_T$ and $\phi_P$ (eq 1 and 5).

*Model Calculations of Lifetime-Resolved Anisotropies.* The interpretation of our data is clarified by first presenting model calculations by using parameters expected for tryptophan residues in proteins. The unquenched fluorescence lifetimes of proteins are near 4 ns. On the average, the lifetime can be decreased to 1 ns by oxygen quenching. We will restrict our model calculations to this range, which illustrates the capabilities and limitations inherent in this quenching method. In these model calculations we also assumed $r_0 = 0.26$, which is the average value we observed for a number of tryptophan residues using an excitation wavelength of 300 nm.

Lifetime-resolved anisotropies are best analyzed by plots of $r^{-1}$ vs. $\tau$. For a tryptophan residue held rigid by the protein matrix ($\alpha = 0$) eq 5 can be rewritten as

$$\frac{1}{r} = \frac{1}{r_0} + \frac{\tau}{r_0\phi_P} \quad (11)$$

A plot of $1/r$ vs. $\tau$ will be linear with an intercept of $1/r_0$ on the $r^{-1}$ axis and a slope of $(r_0\phi_P)^{-1}$. Model calculations for a rigidly held tryptophan residue are shown in Figure 1A. The darker segements of the lines represent the regions where data are available from oxygen quenching, and the lighter sections represent the extrapolations to $\tau = 0$ on the $r^{-1}$ axis. The different lines correspond to different overall correlation times ($\phi_P$). The characteristics of a tryptophan residue held rigidly by the protein matrix are a linear plot of $r^{-1}$ vs. $\tau$ and an intercept on the $r^{-1}$ axis equal to $r_0^{-1}$. Correlation times longer than 20 ns (about 38 000 daltons at 25 °C) are difficult to measure because of the small extent of depolarization due to rotational diffusion.

In Figure 1C we present the contrasting data expected for a highly mobile tryptophan residue ($\phi_T = 0.1$ ns) which is contained in a protein whose rotational correlation time is 20 ns. The extent of the residue motion was varied by changing $\alpha$ from 0 to 1. The lighter lines again represent the anisotropy values expected if the fluorescence lifetime could be quenched to values less than 1 ns. At these shorter lifetimes all the curves intercept the $r^{-1}$ axis at $r_0 = 0.26$, which is the anisotropy of tryptophan in the absence of rotational diffusion.

The dominant effect of a short tryptophan correlation time is a decrease in the apparent $r_0$ value, or more precisely a decrease in $r(0)$. Under favorable circumstances where $\phi_T \ll \phi_P$ and also $\phi_T \ll$ (the minimum quenched lifetime), the extent of the segmental motions can be estimated from the $r_0$ value observed in the absence of rotational motion and the value of $r(0)$ found by extrapolation to $\tau = 0$. Specifically

$$\frac{1}{r} = \frac{1}{r_0(1-\alpha)} + \frac{\tau}{r_0(1-\alpha)\phi_P} \quad (12)$$

Hence, one can use the intercept, $r(0) = r_0(1 - \alpha)$, and the known value of $r_0$ to calculate the average angle for the segmental motion (eq 8). One may expect the rotational correlation time calculated from the slope and intercept to be that

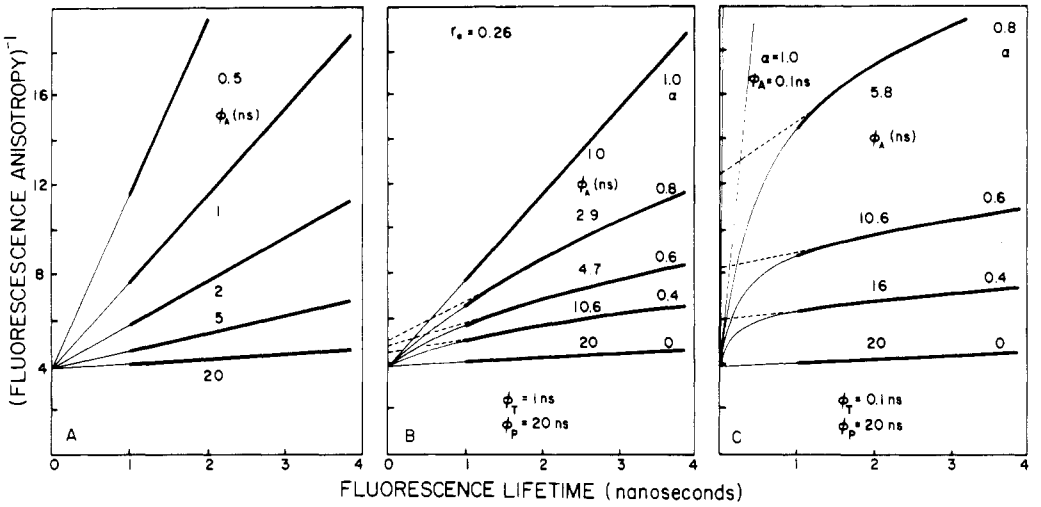


FIGURE 1: Lifetime-resolved anisotropies expected for a tryptophan residue within a protein. The value of $r_0$ is assumed to be 0.26. In part A the value of $\alpha$ is assumed to be zero. In part B the assumed values are $\phi_T$ = 1 ns and $\phi_P$ = 20 ns. In part C $\phi_T$ = 0.1 ns and $\phi_P$ = 20 ns.

of the overall protein rotation. However, we note that even for the extreme values selected for the model calculations in Figure 1C ($\phi_P$ = 20 ns and $\phi_T$ = 0.1 ns), neither the slopes nor the intercept estimated from the limited range of available data precisely reflects $\phi_P$ or the extent of the segmental motion. For example, when $\alpha$ = 0.4 the apparent correlation time ($\phi_A$) estimated from the slope (using the 1–4-ns data) is 16 ns rather than 20 ns. The intercept using these same data yields an apparent $\alpha$ value of 0.36 rather than 0.40. Nonetheless, the existence of the segmental motion is clearly revealed by the low apparent values for $r(0)$ and $\phi_A$. We note that our data did not extend to the curved region of the $r^{-1}$ vs. $\tau$ plots. For this reason we could not determine separate correlation times for the segmental motions and overall rotational diffusion. Apparent correlation times were determined from the available steady-state anisotropies.

Interpretation of the lifetime-resolved anisotropies becomes more ambiguous if the correlation times $\phi_P$ and $\phi_A$ are more comparable. Expected data for $\phi_P$ = 20 ns and $\phi_T$ = 1 ns are shown in Figure 1B. As the extent of the faster motion increases the apparent $r(0)$ values decrease, but less dramatically than in the previous instances where $\phi_T$ = 0.1 ns. For $\phi_T$ = 1 ns, increasing $\alpha$ results in a clear decrease in the apparent correlation time. For example, at $\alpha$ = 0.4, 0.6, and 0.8, the estimated correlation times are 10.6, 4.7, and 2.9 ns, respectively. Clearly, the lifetime-resolved anisotropies alone cannot resolve the precise values of $\phi_P$ and $\phi_T$. This would be possible if the degree of quenching could be extended to shorter lifetimes where curvature in the $r^{-1}$ vs. $\tau$ plots was clearly visible. This was not possible due to the limited solubility of oxygen in aqueous solution. However, even in the absence of such data, the existence of segmental motions can be confidently inferred by observation of either $r(0)$ values which are less than $r_0$ or apparent correlation times which are less than that expected for overall protein rotation.

The average angular displacement of the tryptophan residue, as estimated from $r(0)$, is a minimal estimate. This is apparent from the model calculations. Consider $\alpha$ = 0.8, which corresponds to 80% of the anisotropy being lost by segmental mobility and an angular displacement of 46.9° for the segmental motion. If the $r^{-1}$ intercept accurately revealed the value of $\alpha$, one expects this intercept to be 19.2. However, the model calculations predict intercepts of 5.1 and 12.5 when the residue correlation times are 1 and 0.1 ns, respectively. These intercepts correspond to angles of 24° and 42.8°, respectively. These angles are smaller than the "correct" value. The magnitude of the underestimation is almost 2-fold for reasonable residue correlation times near 1 ns.

For multi-tryptophan proteins the decays of fluorescence anisotropy can be multiexponential because of tryptophan–tryptophan energy transfer, the different fluorescence lifetimes of the individual tryptophan residues, and the different correlation times of these residues. Significant energy transfer among the tryptophan residues is unlikely because of our use of red-edge excitation. Such conditions are known to minimize the extent of energy transfer (Weber, 1960). However, the rotational correlation times among tryptophan residues can differ dramatically (Munro et al., 1979; Lakowicz & Weber, 1980). In contrast the unquenched and quenched lifetimes differ less than several fold (Lakowicz & Weber, 1973b). Consequently, it is most informative to consider the effects of residues with different correlation times on the lifetime-resolved anisotropies. For example, consider a protein with two tryptophan residues. Assume that one residue is completely free to rotate with $\phi_1$ = 1 ns and that the second residue rotates only with the entire protein, $\phi_2$ = 20 ns. The individual anisotropies of these residues can be calculated from eq 5. The measured anisotropy is given by

$$r = r_1 f_1 + r_2 f_2 \qquad (13)$$

where $r_i$ is the individual anisotropies and $f_i$ is the fractional intensities of each residue. Parts B and C of Figure 1 also illustrate the effects of multiple correlation times on the lifetime-resolved anisotropies. For instance, assume $f_1$ = 0.6 and $f_2$ = 0.4. For such a protein the existence of the mobile residue would be revealed by the apparent correlation time, which would be 4.7 ns (Figure 1B). If the rotational rate of the mobile residue were faster ($\phi_T$ = 0.1 ns), then the presence of this rotation would be revealed by the value of $r(0)$ (Figure 1C), which would be smaller than that expected in the absence of rotational diffusion. In the case of multiple tryptophan residues the meaning of the apparent $r_0$ and $\phi_A$ values is complex, but the overall conclusions are similar. Observation of either low apparent values for $r_0$, or correlation times smaller than that expected for overall protein rotation, indicates the presence of segmental motions of at least some of the tryptophan residues.

As indicated above, lifetime-resolved anisotropies can readily reveal the existence of rapid segmental motions of the tryptophan residues. However, it is difficult to resolve the amplitudes and correlation times for these motions because of the limited range of lifetimes which may be obtained by quenching.

However, we note several advantages of the lifetime-resolved measurements. First, with quenchers other than oxygen, no specialized equipment is needed. One relies on the quenching process to achieve time resolution, rather than high-speed detection and electronics, and the potential for error is minimized. Second, steady-state measurements are used, allowing high precision for the individual measurements. Hence, in spite of the limited time resolution, reliable information on the rotational displacements of fluorophores may be obtained.

## Experimental Procedures

*Materials.* RNase $T_1$ and nuclease were gifts from M. Eftink (University of Mississippi), MBP was from F. Prendergast (Mayo Clinic, Minnesota), apo-Hb was from E. Bucci (University of Maryland), and monellin was from R. H. Cagen (Monell Chemical Senses Center, Philadelphia). NATA was obtained from Aldrich. Apoferritin, aldolase, micrococcal nuclease, trypsin, $\alpha$-chymotrypsin, creatinine phosphokinase, alkaline phosphatase, papain, carboxypeptidase A, chorionic gonadotropin, bee venom melittin, and gastrin were from Sigma. The four tripeptides were obtained from Research Plus Chemicals, Denville, NJ, and cosyntropin [adrenocorticotropin-(1–24)] was obtained from Organon, Inc. Pepsin and a second sample of MBP were from Calbiochem. All the above materials were used without further purification. Rechromatographed HSA was obtained from Worthington and further purified by gel filtration on Sephacell 200 using 0.1 M sodium phosphate, pH 7.5, as the eluent. LADH was obtained from Boehringer-Mannheim as a crystalline suspension. Prior to use LADH was dialyzed 48 h against buffer, centrifuged to removed undissolved protein and diluted to yield an optical density near 0.1 at 300 nm. Samples which displayed visible turbidity, probably due to self-association (Ross et al., 1979), were not used. For all quenching and phase lifetime measurements the protein and peptide concentrations were adjusted to yield optical densities near 0.3 at 295 nm.

*Oxygen Quenching.* Stern–Volmer quenching constants ($K = k_q\tau_0$) were obtained from

$$\frac{F_0}{F} = 1 + K[O_2] \tag{14}$$

where $F_0$ and $F$ are the total fluorescence intensities in the absence and presence of quencher, respectively, and $\tau_0$ is the lifetime in the absence of quencher. The bimolecular quenching constant ($k_q$) is then calculated from $K$ and $\tau_0$. The oxygen concentrations are given by Henry's law by using the known solubilities of oxygen in water of one atmosphere of pressure. These temperature-dependent values were obtained by interpolation by using the values given previously (Lakowicz & Weber, 1973a).

*Lifetime-Resolved Anisotropies.* Fluorescence anisotropy measurements of samples equilibrated with increased pressures of oxygen were performed as described previously (Lakowicz et al., 1979; Lakowicz & Weber, 1980). Excitation was at 300 nm to provide both a high limiting anisotropy ($r_0$) and to avoid excitation of tyrosine residues. An excitation filter (Corning 7-54) was used to decrease stray light. So that the precise optical conditions which were used for the lifetime measurements could be matched, the excitation slits were adjusted to 8 and 2 nm, with the former value describing the slit closest to the light source. Anisotropies were measured at an emission wavelength of 344 nm, with an emission band-pass of 8 nm. Anisotropies were calculated from

$$r = \frac{I_\parallel G - I_\perp}{I_\parallel G + 2I_\perp} \tag{15}$$

where $G$ is the correction factor for the monochromator's efficiency in the transmission of vertically and horizontally polarized light. This value is given by the ratio of the fluorescence intensities of the horizontally to the vertically polarized components when the exciting light is polarized in the horizontal direction. The total fluorescence intensity, which is necessary for determination of the extent of quenching, is given by

$$F = I_\parallel G + 2I_\perp \tag{16}$$

In our instruments the $G$ factor cannot be determined by using the same excitation wavelength as for the anisotropy measurements (300 nm). This situation is a result of the complete vertical polarization of the light exiting the monochromator at this wavelength. We circumvented this problem by determining the $G$ factor using excitation wavelengths of 280, 285, 290, and 295 nm and averaging the results. The $G$ value is a characteristic of the detection system and is hence independent of excitation wavelength. As expected, similar values were obtained at the four excitation wavelengths. These values were averaged to improve precision.

*Fluorescence Lifetimes.* These values were measured under similar conditions except that the excitation wavelength was 295 nm and the emission was observed through an interference filter centered at 344 nm. The excitation was polarized vertically and the emission at 54.7° from the vertical. This eliminates the effects of Brownian rotation on the measured lifetimes (Spencer & Weber, 1970). Lifetimes were measured by the phase shift method (Spencer & Weber, 1969) with a modulation frequency of 30 MHz. We used *p*-terphenyl or PPD (2,5-diphenyl-1,3,4-oxadiazole) in ethanol in place of the usual glycogen scatterer and reference lifetimes of 1.0 and 1.2 ns, respectively. This procedure corrects for the wavelength and geometry dependent time response of the photomultiplier tubes (Lakowicz et al., 1981).

In all experiments excitation was on the red edge of the absorption band. Such conditions decrease the amount of light absorbed by the fluorophore and increase the possiblity of contributions from fluorescent impurities and scattered light. For this reason we carefully examined blank spectra of the buffers. In all instances background fluorescence accounted for less than 2% of the total fluorescence. These determinations were done with both polarizers in the vertical position to maximize the possible contributions due to scattered light.

## Results

*Determination of the Anisotropy in the Absence of Rotational Diffusion.* Interpretation of the lifetime-resolved anisotropy data requires knowledge of the anisotropy in the absence of rotational displacements. As described under Theory one cannot simply extrapolate to zero lifetime because rapid motions may be unresolved, resulting in low extrapolated values for $r(0)$. However, if $r_0$ could be estimated for the tryptophan residues, then one could interpret the intercepts on the $1/r$ axis [$r(0)$] in terms of the angular freedom of rapid unresolved rotational motions (eq 8).

We examined the $r_0$ values in detail, the object being to assign the value expected at $\tau = 0$ if segmented motions were not present. Our reasoning was that the limiting anisotropy was likely to be determined by the electronic properties of the chromophore, and hence be similar for all proteins and peptides. We examined the excitation polarization spectra of most of the single tryptophan compounds used in this study, over the wavelength range from 295 to 305 nm. These measurements were performed in solutions consisting of 70% propylene glycol/30% buffer. The temperature was decreased to −58

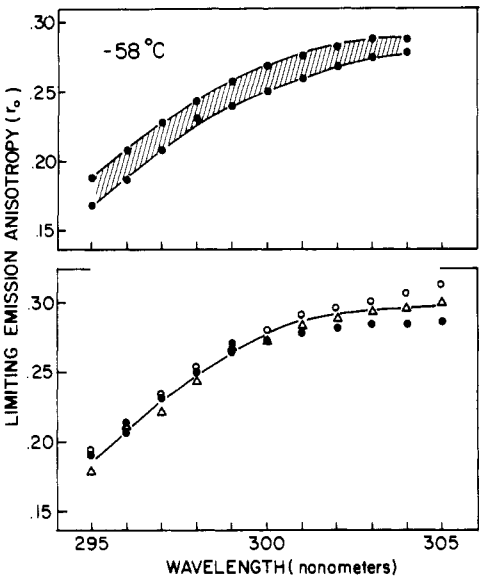


FIGURE 2: Limiting anisotropies ($r_0$) for protein and peptides. (Top) The lines indicate the highest and lowest values observed among the single tryptophan compounds listed in Table I. (Bottom) Data are shown for NATA in glycerol (○), propanediol (△), and propanediol/buffer (70/30) (●).

Table I: Limiting Anisotropies ($r_0$) Observed in Vitrified Solution

| compound (solvent)[a] | $r_0$ (295 nm) | $r_0$ (300 nm) |
|---|---|---|
| NATA (glycerol) | 0.194 | 0.280 |
| NATA (1,2-propanediol) | 0.179 | 0.273 |
| NATA (a) | 0.191 | 0.273 |
| Gly-Trp-Gly (a) | 0.175 | 0.257 |
| Leu-Trp-Leu (a) | 0.182 | 0.262 |
| Glu-Trp-Glu (a) | 0.171 | 0.262 |
| Lys-Trp-Lys (a) | 0.174 | 0.260 |
| gastrin (a) | 0.170 | 0.255 |
| cosyntropin (a) | 0.172 | 0.261 |
| glucagon (b) | 0.171 | 0.263 |
| melittin (c) | 0.172 | 0.260 |
| +1.5 M NaCl | 0.175 | 0.259 |
| monellin (d) | 0.168 | 0.259 |
| monellin (e) | 0.183 | 0.269 |
| (e) + 5 M Gdn·HCl | 0.187 | 0.262 |
| HSA (a) | 0.167 | 0.251 |

[a] Limiting anisotropies were measured in the same buffers used for oxygen quenching (see Table II), except that these solutions (3 volumes) were mixed with 1,2-propanediol (7 volumes) and then cooled to −58 °C. NATA was examined both in the buffer-propanediol mixture, in pure propanediol, and in pure glycerol.

°C to inhibit rotational diffusion. The similarity among these data is striking, as is shown in Table I and Figure 2. In the upper panel of Figure 2 we show the $r_0$ values measured for a number of single tryptophan peptides and proteins (Table I) in 70% propylene glycol at −58 °C. The lines represent the extreme upper and lower values found among the compounds listed in Table I. The $r_0$ values for all these compounds are within experimental error. In addition, we examined the effect of different vitrifying solvents on the limiting anisotropies of NATA (lower panel of Figure 2). Only minor differences in the $r_0$ values were observed in glycerol, propylene glycol, and propylene glycol/water, 70/30. The origin of these small differences is unknown. Possibilities included differing microscopic viscosities at −58 °C or solvent-induced shifts in the absorption spectrum. In any event, the marked similarity of the excitation polarization spectra for these compounds clearly justifies the choice of a single value for $r_0$ at any given excitation wavelength and band-pass where tryptophan is the only

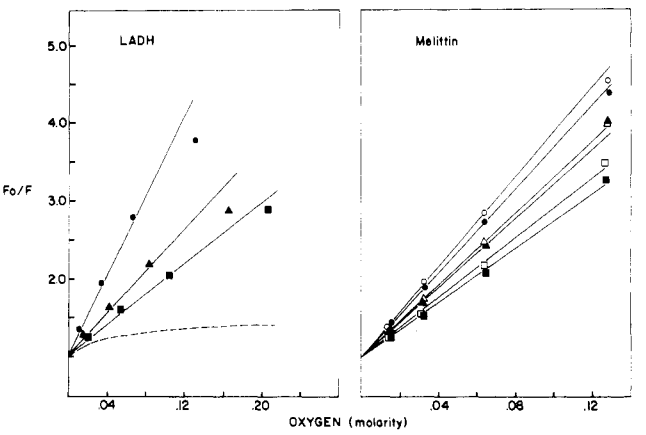


FIGURE 3: Stern–Volmer plot for oxygen quenching of LADH and melittin. For LADH the oxygen quenching was measured at 3 (■), 12 (▲), and 24 °C (●). The dashed line indicates the quenching expected for a protein containing two tryptophan residues, one of which is 100-fold less accessible to oxygen. Increasing concentrations of NaCl cause melittin to form tetramers. The salt concentrations are 0 (○), 0.15 (●), 0.3 (△), 0.6 (▲), 0.5 (□), and 2.4 M (■), 25 °C.

Table II: Unquenched Fluorescence Lifetimes and Oxygen Quenching Constants for Single Tryptophan Peptides and Proteins

| compound (solvent)[a] | temp (°C) | $\tau_0$ (ns) | $K$ ($M^{-1}$) | $k_q \times 10^{-10}$ ($M^{-1}$ $s^{-1}$) |
|---|---|---|---|---|
| NATA (a) | 23 | 2.73 | 37.1 | 1.36 |
| Gly-Trp-Gly (a) | 23 | 1.55 | 15.5 | 1.0 |
| Leu-Trp-Leu (a) | 23 | 2.32 | 23.2 | 1.0 |
| Glu-Trp-Glu (a) | 23 | 1.71 | 16.8 | 0.98 |
| Lys-Trp-Lys (a) | 23 | 2.24 | 22.4 | 1.0 |
| gastrin (a) | 23 | 3.45 | 38.0 | 1.10 |
| cosyntropin (a) | 23 | 2.88 | 20.2 | 0.75 |
| glucagon (b) | 23 | 2.54 | 22.4 | 0.88 |
| melittin (c) | 25 | 2.60 | 28.6 | 1.10 |
| +0.15 M NaCl | 25 | 2.52 | 27.2 | 1.08 |
| +0.3 M NaCl | 25 | 2.48 | 23.3 | 0.94 |
| +0.6 M NaCl | 25 | 2.37 | 22.5 | 0.95 |
| +1.5 M NaCl | 25 | 2.34 | 19.4 | 0.83 |
| +2.4 M NaCl | 25 | 2.15 | 17.6 | 0.82 |
| monellin (d) | 25 | 2.45 | 18.9 | 0.77 |
| monellin (e) | 25 | 2.67 | 16.0 | 0.60 |
| (e) +1 M Gdn·HCl | 25 | 2.36 | 13.7 | 0.58 |
| (e) +2 M Gdn·HCl | 25 | 2.33 | 13.3 | 0.57 |
| (e) +5 M Gdn·HCl | 25 | 1.76 | 12.0 | 0.68 (1.30)[b] |
| myelin basic protein (f) | 5 | 3.76 | 15.8 | 0.42 |
| | 20 | 3.03 | 17.9 | 0.59 |
| | 35 | 2.12 | 19.1 | 0.90 |
| chorionic gonadotropin (g) | 25 | 3.02 | 17.1 | 0.56 |
| RNase $T_1$ (g) | 25 | 3.75 | 8.1 | 0.21 |
| nuclease (h) | 20 | 4.10 | 4.1 | 0.42 |
| HSA (a) | 5 | 4.55 | 9.1 | 0.20 |
| | 18 | 4.18 | 9.6 | 0.23 |
| | 30 | 3.79 | 14.8 | 0.39 |
| | 44 | 3.39 | 18.3 | 0.54 |
| HSA | 5 | 3.78 | 7.8 | 0.21 (0.40)[b] |
| +6 M Gdn·HCl | 18 | 3.26 | 8.8 | 0.27 (0.52) |
| | 30 | 2.62 | 8.7 | 0.33 (0.64) |
| | 44 | 1.94 | 14.8 | 0.76 (1.47) |

[a] The solvents used were as follows: a, 0.1 M sodium phosphate, pH 7.5; b, aqueous HCl, pH 2.4; c, 0.02 M Tris–acetate and 0.2 mM EDTA, pH 7.5; d, 0.02 M sodium phosphate, pH 7.5; e, 0.1 M acetate, pH 3.6; f, 0.05 M sodium phosphate and 0.15 M NaCl, pH 7.4; g, 0.05 M sodium phosphate, pH 7.5; h, 0.1 M Tris-HCl and 10 mM $CaCl_2$, pH 8.0. [b] The values in parentheses are corrected for the effect of 5 M guanidine hydrochloride on the observed oxygen quenching (Lakowicz & Weber, 1973b). The other values for monellin are not corrected for these effects.

absorbing species. From these data we selected an $r_0$ value at 300-nm excitation of 0.260.

*Oxygen Quenching of Proteins and Peptides.* Typical Stern–Volmer plots are shown in Figure 3, and the Stern–

Table III: Unquenched Fluorescence Lifetimes and Oxygen Quenching Constants for Multi-Tryptophan Proteins

| protein (solvent)[a] | temp (°C) | $\tau_0$ (ns) | $K$ ($M^{-1}$) | $k_q \times 10^{-10}$ ($M^{-1}$ $s^{-1}$) |
|---|---|---|---|---|
| alkaline phosphatase (d) | 25 | 3.23 | 5.5 | 0.17 |
| LADH (a) | 3 | 4.95 | 9.9 | 0.20 |
| | 12 | 4.70 | 13.6 | 0.29 |
| | 24 | 4.36 | 25.7 | 0.59 |
| aldolase (e) | 25 | 1.55 | 5.7 | 0.37 |
| apoferritin (e) | 25 | 1.39 | 5.4 | 0.39 |
| creatine phosphokinase (c) | 25 | 2.12 | 8.4 | 0.40 |
| carboxypeptidase A (f) | 25 | 1.59 | 7.4 | 0.46 |
| pepsin (b) | 25 | 5.05 | 24.8 | 0.49 |
| apo-Hb (a) | 5 | 2.94 | 16.5 | 0.56 |
| papain (e) | 25 | 3.95 | 22.8 | 0.58 |

[a] Solvents: a, 0.1 M phosphate buffer, pH 7.5; b, 0.01 M HCl; c, 0.10 M Tris buffer, pH 7.5; d, 0.5 M Tris buffer, pH 8.0; e, 0.05 M phosphate buffer, pH 7.5; f, 0.02 M Tris buffer containing 0.5 M NaCl, pH 7.5.

Volmer quenching constants and lifetimes are summarized in Tables II and III. Several general features of these data are worthy of mention. The Stern–Volmer plots were linear to within our experimental error. This indicates that static quenching was not significant and that no significant fraction of the tryptophan fluorescence is inaccessible to quenching. Previously we demonstrated, for a variety of different fluorophores and proteins, that the observed quenching was due to diffusional quenching which shortens the lifetime in proportion to the decrease in the fluorescence yield (Lakowicz & Weber, 1973a,b). The quenching constants of NATA, the four tripeptides, cosyntropin, gastrin, glucagon, and melittin are all near the value expected for tryptophan residues which are exposed to the aqueous phase. For diffusion-controlled quenching of an unshielded residue this value is near $1.2 \times 10^{10}$ $M^{-1}$ $s^{-1}$. As the size of the proteins increase some shielding of the tryptophan residues was observed (Tables II and III). Glucagon and cosyntropin each show some shielding of the residues, which is perhaps consistent with a partially ordered structure around the tryptophan residue. For the remaining proteins the bimolecular quenching constants range from 20 to 80% of the diffusion-controlled values, which is comparable to that found previously for native proteins (Lakowicz & Weber, 1973b). These data (Tables II and III) confirm our earlier conclusions which indicate the accessibility of all tryptophan residues in proteins to collisional encounters with oxygen. Denaturation of HSA and monellin was found to increase the bimolecular quenching constants to values comparable to those of the smaller peptides. Hence, the structures of native proteins do partially shield the tryptophan residues from collisions with oxygen, but the extent of shielding is small. Surprisingly, the data for MBP at lower temperature (5 and 20 °C) indicate some shielding of the tryptophan residue from oxygen. These results are consistent with the NMR data, which suggest that even though MBP exists predominately as a random coil, some structure exists in the region surrounding the tryptophan residue (Chapman & Moore, 1976, 1978).

Several of the data sets were chosen for explicit presentation because of their potential importance. Figure 3 (left panel) shows our data for the quenching of LADH. LADH has four subunits, each of which contains two tryptophan residues. One residue appears to be deep within a subunit and the second exposed to the aqueous phase (Abdallah et al., 1978; Barboy & Feitelson, 1978; Ross et al., 1981b). We used 300-nm excitation, a condition which results in partial selective excitation of the internal tryptophan residue (Purkey & Galley, 1970). From our data we calculate a quenching constant of $0.2 \times 10^{10}$ $M^{-1}$ $s^{-1}$ at 3 °C, with still larger values being observed at 12 and 24 °C (Table II). The modest downward curvature of the Stern–Volmer plots for LADH (Figure 3) does not indicate the presence of an unquenchable tryptophan but perhaps reflects a somewhat less accessible residue. The downward deviation of the last data points in Figure 3 (left panel) is comparable to our experimental accuracy, and we do not wish to interpret this minor effect. Similar results were found by Eftink & Jameson (1982). The dashed line in Figure 3 models the quenching expected for two populations, one of which is 100-fold less accessible to quenching. The quenching constants were assumed to be $K_1 = 42$ $M^{-1}$ and $K_2 = 0.23$ $M^{-1}$, and the fractional intensity of the internal residue was assumed to be 0.7. These values were chosen by using our oxygen bimolecular quenching constant at 24 °C, the lifetimes given by Ross et al. (1981b), and the fractional intensities and relative accessibilities given by Eftink & Selvidge (1982). Clearly, if a residue were inaccessible to oxygen, this fact would have been revealed by the Stern–Volmer plot. We cannot explain the lack of phosphorescence quenching by oxygen observed by Savioti & Galley (1974). However, we note that our results are consistent with those of Vanderkooi et al. (1982) and Eftink & Jameson (1982), who found that the internal tryptophan of LADH is accessible to oxygen quenching of both the fluorescence and phosphorescence of LADH.

As a second example we chose to present our quenching data for melittin in the presence of varying concentrations of sodium chloride. Melittin is known to self-associate at high ionic strength to form tetramers (Talbot et al., 1979; Faucon et al., 1979). Self-association is accompanied by a blue shift in the fluorescence emission from 352 to 337 nm, which is indicative of partial shielding of the tryptophan residue from the aqueous phase. Our fluorescence spectra at various concentrations of sodium chloride were essentially equivalent to those described earlier (Talbot et al., 1979). The Stern–Volmer plots are shown in Figure 3 (right panel). Increased salt concentration results in a small decrease in the bimolecular quenching constant from $1.1 \times 10^{10}$ to $0.82 \times 10^{10}$ $M^{-1}$ $s^{-1}$. We note that these values were not corrected for the effect of the increased salt concentration on the oxygen solubility and diffusion coefficient. Irrespective of this consideration, it is clear that the tryptophan residues are still highly accessible to collisional encounters with oxygen.

*Lifetime-Resolved Fluorescence Anisotropies of Small Peptides.* Lifetime-resolved anisotropies are measured by steady-state methods, a fact which allows considerable precision in the individual measurements. This point is illustrated by our results with NATA, the tripeptides, and gastrin tetrapeptide, which is Trp-Met-Asp-Phe-$NH_2$. Because of the low molecular weight and the resulting high rates of rotational diffusion, the fluorescence anisotropies are quite low. For example, for NATA equilibrated with 0 and 1469 psi of $O_2$, the anisotropies are 0.0047 and 0.0279, respectively. Nonetheless, these small changes in anisotropy are adequate to obtain a reasonable estimate of the rotational correlation time, which we estimated to be 0.03 ns. This value is in agreement with the rotational correlation time for NATA determined by using viscosity variation and extrapolation to low viscosity (Bernstein et al., 1969) and with the value estimated by Munro et al. (1979). This value is somewhat smaller than expected on the basis of its molecular weight. The smaller value of the rotational correlation time is probably a result of diffusive motion of the indole side chain independent of the polar side

Table IV: Tryptophan Correlation Times and $r(0)$ Values for the Single Tryptophan Peptides and Proteins

| compound | temp (°C) | $\phi_A$ (ns) | $\phi_P$ (ns) | $r(0)$ | $\phi_P/\phi_A$ [b] | $r_0/r(0)$ | $\theta_T$ (deg) |
|---|---|---|---|---|---|---|---|
| NATA | 23 | 0.03 | 0.13 | [a] | 4.33 | | |
| Gly-Trp-Gly | 23 | 0.12 | 0.17 | [a] | 1.42 | | |
| Leu-Trp-Leu | 23 | 0.12 | 0.20 | [a] | 1.67 | | |
| Glu-Trp-Glu | 23 | 0.14 | 0.20 | [a] | 1.43 | | |
| Lys-Trp-Lys | 23 | 0.19 | 0.20 | [a] | 1.05 | | |
| gastrin | 23 | 0.14 | 0.33 | [a] | 2.36 | | |
| cosyntropin | 23 | 1.22 | 1.55 | 0.18 | 1.27 | 1.44 | 27 |
| glucagon | 23 | 1.20 | 1.91 | 0.18 | 1.59 | 1.44 | 27 |
| melittin | 25 | 1.18 | 1.85[c] | 0.152 | 1.57 | 1.71 | 32 |
| +0.15 M NaCl | 25 | 1.83 | | 0.151 | | 1.72 | 32 |
| +0.3 M NaCl | 25 | 2.55 | | 0.159 | | 1.64 | 31 |
| +0.6 M NaCl | 25 | 2.90 | | 0.165 | | 1.58 | 30 |
| +1.5 M NaCl | 25 | 3.42 | | 0.163 | | 1.60 | 30 |
| +2.4 M NaCl | 25 | 3.76 | 7.42[c] | 0.153 | 1.97 | 1.70 | 32 |
| monellin (d) | 25 | 6.08 | 5.7 | 0.210 | 0.94 | 1.24 | 21 |
| monellin (e) | 25 | 5.78 | | 0.231 | | 1.13 | 16 |
| (e) + 1 M Gdn·HCl[d] | 25 | 6.45 | | 0.218 | | 1.19 | 19 |
| (e) + 2 M Gdn·HCl | 25 | 4.79 | | 0.176 | | 1.48 | 28 |
| (e) + 5 M Gdn·HCl | 25 | 1.76 | 3.65[e] | 0.140 | 2.07 | 1.86 | 34 |
| myelin basic protein | 5 | 3.52 | 17.8 | 0.20 | 5.06 | 1.30 | 23 |
| | 20 | 2.60 | 11.2 | 0.18 | 4.31 | 1.44 | 27 |
| | 35 | 1.73 | 7.6 | 0.17 | 4.41 | 1.53 | 29 |
| chorionic gonadotropin | 25 | 8.00 | 28.6 | 0.208 | 3.60 | 1.25 | 21 |
| RNase $T_1$ | 25 | 5.9 | 5.8 | 0.264 | 1.0 | 1.0 | 0 |
| nuclease | 20 | 8.7 | 10.5 | 0.244 | 1.19 | 1.05 | 10 |
| HSA | 5 | 44.6 | 66.6 | 0.262 | 1.49 | 0.99 | 0 |
| | 18 | 22.4 | 44.2 | 0.260 | 1.97 | 1.00 | 0 |
| | 30 | 16.9 | 32.2 | 0.250 | 1.90 | 1.04 | 9 |
| | 44 | 8.5 | 23.5 | 0.260 | 2.77 | 1.00 | 0 |
| HSA | 5 | 4.4 | 108 | 0.213 | 25.5 | 1.22 | 20 |
| +6 M Gdn·HCl | 18 | 2.9 | 71.5 | 0.192 | 28.7 | 1.35 | 25 |
| | 44 | 1.5 | 38.0 | 0.169 | 25.9 | 1.54 | 29 |

[a] Because of the short correlation times the extrapolation of $r^{-1}$ to $\tau = 0$ is subject to considerable uncertainty. All the apparent intercepts were near 0.25, but small changes in the chosen extrapolation result in large changes in the intercept $[r(0)]^{-1}$. [b] This number is the ratio of the calculated correlation times. [c] These values are for the monomer and the tetramer. [d] The relative viscosities of aqueous solution of guanidine hydrochloride were estimated from the *Handbook of Biochemistry* (1970). [e] To calculate this value we assumed that 5 M Gdn·HCl dissociated monellin into subunits and that the molecular weight of the tryptophan-containing subunit was 4900.

chain and the failure of the Stokes–Einstein equation (with stick boundary conditions) to predict the correlation time of molecules whose size is comparable to that of the solvent molecules (Mantulin & Weber, 1977). Rather short correlation times were also found for the four tripeptides and for gastrin (Figure 4 and Table IV). The measured values are somewhat smaller than that expected for a rigid molecule of equivalent molecular weight. The discrepancy is slight but again probably a result of rotational freedom of the indole residue around the carbon bond linking it to the peptide backbone. Since the tryptophan residue in gastrin is at the N-terminal position, it is not surprising that the correlation time of this residue is smaller than that expected for a rigid sphere. Moreover, NMR data indicate that the aromatic residues Trp and Phe are well separated in gastrin, indicating an extended structure in aqueous solution (Feeney et al., 1972).

For the smaller peptides the extent of depolarization is high even at the shortest quenched lifetimes. As a result the extrapolation to zero lifetime, which is necessary for the determination of $r(0)$, is highly variable. For NATA, the tripeptides, and gastrin, the apparent $r(0)$ values appear to be near 0.25. However, small changes in the line drawn through the available data result in markedly different $r(0)$ values. For this reason these values are not liseted in Table IV.

Similar data were obtained for cosyntropin ($M_r$ 2934) and glucagon ($M_r$ 3600). In these cases the apparent $\phi_A$ values are comparable to those expected for the rigid spheres (Table IV). As described under Theory the separation of the correlation times due to overall rotation and residue motion is difficult when these values are comparable. However, evidence for excess rotational freedom of the tryptophan residues is

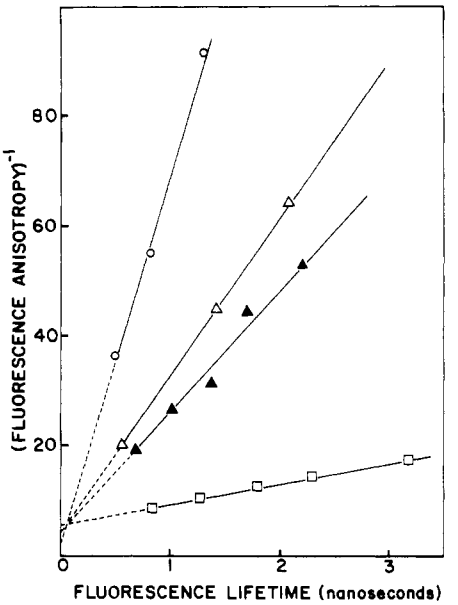


FIGURE 4: Lifetime-resolved anisotropies for several small peptide data are shown for NATA (○), gastrin (△), Glu-Trp-Glu (▲), and glucagon (■).

provided by the extrapolation to zero lifetime. These $r(0)$ values (0.18) are significantly less than the value expected for an immobile trytophan residue (0.26). Under the assumption that this excess motion is much faster than protein rotation, the loss in anisotropy corresponds to independent rotation of the tryptophan residues through an angle of 27° (eq 8). This

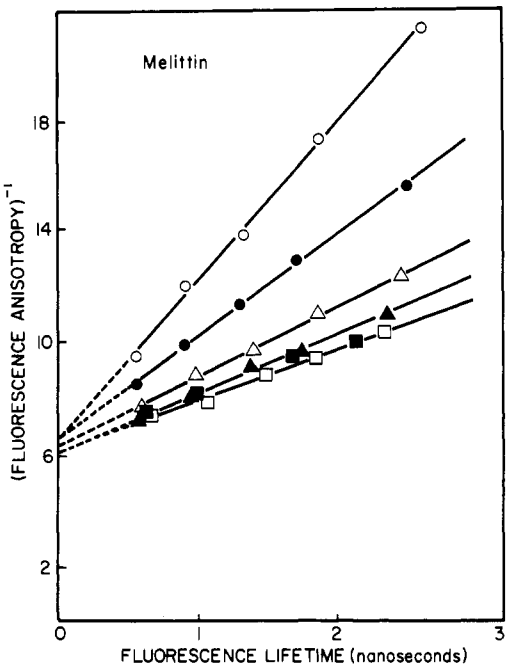


FIGURE 5: Effects of self-association of melittin on the tryptophan correlation times, 25 °C. Salt concentrations are listed in the legend of Figure 3.

angle is the minimal estimate of the degree of freedom, as was described under Theory.

*Effects of Self-Association on the Tryptophan Correlation Times of Melittin.* We examined the lifetime-resolved anisotropies of melittin at various salt concentrations (Figure 5). At low salt concentration where melittin is monomeric the apparent correlation time was 1.2 ns, somewhat smaller than that expected for the rigid hydrated sphere. This observation, in combination with the low value of $r(0)$ (Table IV), indicates some rotational freedom of this residue in excess of overall protein rotation. Self-association results in an approximate 4-fold increase in $\phi_A$, as would be expected for tetramer formation. The precision of these measurements is illustrated by the monotonic increase in $\phi_A$ with increasing salt concentration. Only a small increase in the $r(0)$ value is seen upon self-association, suggesting that the tryptophan residue still has considerable rotational freedom in the tetramer. The correlation times observed at 0 and 2.4 M NaCl are in excellent agreement with those found by Georghiou et al. (1981) when time-resolved decays of fluorescence anisotropy were used. In agreement with our results, Georghiou et al. also found evidence for a unresolved segmental motion of the tryptophan residue, as evidence by a anisotropy of 0.16 for $t = 0$.

*Myelin Basic Protein.* Earlier studies using time-resolved decays of fluorescence anisotropy indicated that the single tryptophan residue in MBP was highly mobile (Munro et al., 1979). We also found significant mobility of this residue in excess of overall protein rotation (Figure 6 and Table IV). The measured correlation times (1.7–3.5 ns) were substantially smaller than that expected for the rigid sphere (11 ns), and the $r(0)$ values indicate motions of these residues which are faster than our shortest quenched lifetimes ($\simeq$1 ns). Our measured $\phi_A$ values are probably consistent with a small amount of structure around the tryptophan residue (Chapman & Moore, 1976, 1978). Our results are in qualitative agreement with those of Munro et al. (1979) in that the tryptophan residue is mobile relative to the protein. However, the quantitative agreement is poor. In Figure 6 we illustrate

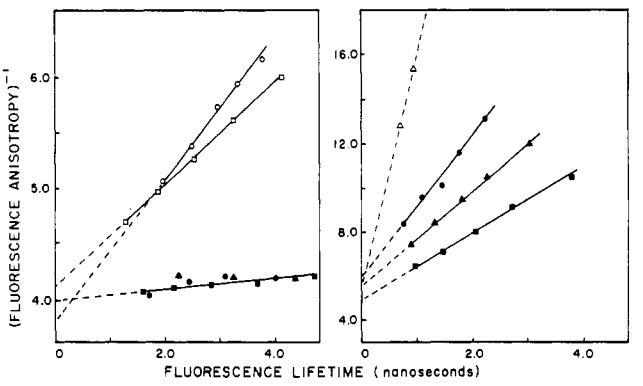


FIGURE 6: Lifetime-resolved anisotropies of RNase $T_1$, nuclease, LADH, and myelin basic protein. (Left panel) for RNase $T_1$ (○) and nuclease (□) the temperatures were 25 and 20 °C, respectively. For LADH the temperatures were 3 (■), 12 (▲), and 24 (●) °C. (Right panel) Myelin basic protein at 5 (■), 20 (▲), and 35 (●) °C. The dashed line shows the values expected from the results of Munro et al. (1979) for myelin basic protein.

the result expected (broken line) on the basis of their results. To predict these values we used eq 10 and the published parameters ($\alpha_1 = 0.15$, $\phi_1 = 0.09$ ns, $\alpha_2 = 0.106$, and $\phi_2 = 1.26$). Clearly, the predicted anisotropies and the expected apparent correlation time are both substantially smaller than our measured values. The reason for this marked discrepancy is unknown. Our solution conditions are identical with those reported by Munro et al. (1979). We have examined two different preparation of MBP and found similar results for each.

*Nuclease and RNase $T_1$.* We also examined the native single tryptophan proteins, nuclease, and RNase $T_1$. In both cases the apparent correlation times were comparable to that expected for overall protein rotation (Table IV), and the $r(0)$ values were indicative of largely immobilized tryptophan residues. Our results for nuclease are in agreement with the time-resolved studies of Munro et al. (1979), who also found a correlation time comparable to that expected for overall protein rotation.

*Liver Alcohol Dehydrogenase.* The two tryptophan residues of LADH were found to be completely immobilized by the protein matrix (Figure 6 and Table V). Because of the large molecular weight of LADH, there is little loss of anisotropy during the lifetime of the excited state. As a result the correlation times of LADH listed in Table V are subject to considerable uncertainty. However, the lack of free tryptophan rotation is well demonstrated by $r(0) = 0.26$. These results are in good agreement with the time-resolved studies of Ross et al. (1981b), who found that both the internal and external residues of LADH rotated with the protein as a whole.

*Effects of Denaturation on the Tryptophan Correlation Times of Monellin and Human Serum Albumin.* We examined the effects of denaturation by guanidine hydrochloride on the correlation times of the tryptophan residues in monellin and HSA. At low temperature, the single tryptophan residue in HSA appears to be rigidly held within the protein matrix, as indicated by both the corelation time of 44 ns and the $r(0)$ value of 0.26. Increasing temperature results in some freedom of tryptophan rotation, which is in qualitative agreement with the results of Munro et al. (1979). The apparent correlation times for monellin are comparable to that expected for a rigid sphere. However, the presence of internal motions is suggested by the low values of $r(0)$ (Figure 7 and Table IV). Such motion may be expected since the tryptophan residue is located at the third position from the N-terminal end of the smaller monellin subunit (Bohak & Li, 1976).

Table V: Correlation Times and $r(0)$ Values for Tryptophan Residues in Multi-Tryptophan Proteins[a]

| protein | temp (°C) | $\phi_A$ (ns) | $\phi_P$ (ns) | $r(0)$ | $\phi_P/\phi_A$ | $r_0/r(0)$ | $\theta_T$ (deg) |
|---|---|---|---|---|---|---|---|
| alkaline phosphatase | 25 | 21.3 | 44.5 | 0.250 | 2.1 | 1.04 | 9 |
| LADH[b] | 3 | | 85.9 | 0.260 | | 1.00 | 0 |
| | 12 | 74.0 | 61.3 | 0.260 | 0.83 | 1.00 | 0 |
| | 24 | | 43.4 | 0.260 | | 1.00 | 0 |
| aldolase | 25 | 52.0 | 85 | 0.271 | 1.6 | 0.96 | |
| apoferritin | 25 | 9.6 | 250 | 0.238 | | 1.09 | 14 |
| creatine phosphokinase | 25 | 13.8 | 43.5 | 0.227 | 3.2 | 1.15 | 17 |
| carboxypeptidase A | 25 | 6.2 | 18.5 | 0.182 | 3.0 | 1.43 | 27 |
| pepsin | 25 | 10.4 | 18.5 | 0.230 | 1.8 | 1.13 | 16 |
| apo-Hb | 5 | 31.0 | 32.0[c] | 0.232 | 1.0 | 1.12 | 16 |
| papain | 25 | 4.5 | 12.2 | 0.116 | 2.7 | 2.24 | 37 |

[a] The buffers used are listed in Table III. [b] This is the average value observed for 3, 12, and 24 °C. [c] The dominant species was assumed to be a $\alpha\beta$ dimer.

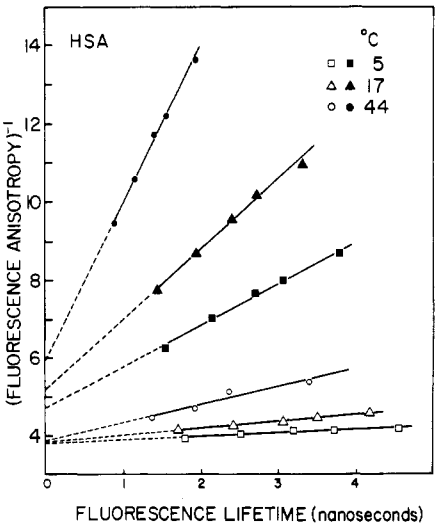


FIGURE 7: Effect of denaturation on the lifetime-resolved anisotropies of human serum albumin. The closed symbols refer to denatured protein (6 M guanidine hydrochloride), and the open symbols refer to native protein.

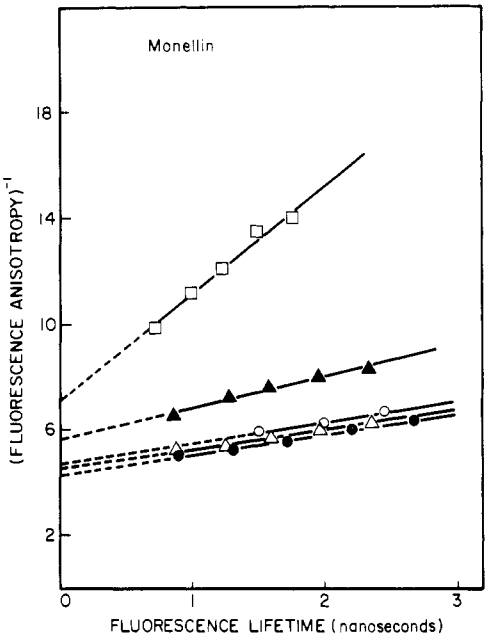


FIGURE 8: Effects of guanidine hydrochloride on the lifetime-resolved anisotropies of monellin. Data are shown in 0.02 M phosphate, pH 7.5 (○), 0.1 M acetate, pH 3.6 (●), and 0.1 M acetate, pH 3.6, containing 1 (△), 2 (▲), and 5 (□) M guanidine hydrochloride.

Denaturation of both monellin and HSA resulted in a substantial decreases in the $\phi_A$ values and decreases in $r(0)$. For example, the $\phi_A$ value for HSA decreases from 44 to 4.4 ns, and the $r(0)$ value decreases from 0.26 to 0.213. Hence the rotational freedom is increased upon denaturation. Similar results were obtained for monellin (Figure 8), where denaturation results in a decrease of $\phi_A$ from 5.8 to 1.8 ns and a decrease in $r(0)$ from 0.21 to 0.14. Of course, some of this decrease in $\phi_A$ could be a result of dissociation of monellin into its subunits. It is interesting to note that 1 M Gdn·HCl had no detectable effect on the tryptophan dynamics. Brand & Cagan (1977) have shown that monellin was denatured in a stepwise manner near a guanidine concentration of 0.5 M.

*Multi-Tryptophan Proteins.* We also examined a number of proteins which contained more than a single tryptophan residue (Table V). The tryptophan residues of these proteins displayed variable degrees of segmental mobility. In some cases we found apparent correlation times which were smaller than that expected for overall protein rotation and small values for $r(0)$. In contrast, the tryptophan residues in LADH and aldolase were found to be immobile. Hence, in multi-tryptophan proteins, one expects the presence of both free and mobile residues. On the average, some segmental mobility will be observed, and the data summarized in Table V probably represents an average of these different motions.

Among the multi-tryptophan proteins papain is unique with respect to both the short apparent correlation time and the low value of $r(0)$ (Table V and Figure 9). These results seem to indicate a remarkable degree of freedom for the five tryptophan residues. However, earlier studies have shown that the fluorescence of papain is dominated by a single tryptophan residue which accounts for about 60% of the total fluorescence at pH 7.5 (Steiner, 1971). From its red-shifted emission spectrum, this residue is throught to be exposed to the aqueous phase and near the catalytic site of the protein. Hence the high degree of flexibility indicated from our studies is probably indicative of the dynamics of this residue, and not necessarily the entire protein.

## Discussion

In the previous sections we described the use of steady-state anisotropy measurements, under conditions of oxygen quenching, to determine the rotational correlation times of tryptophan residues in peptides and proteins. A wide range of peptides and proteins were investigated, and in some cases the experimental conditions were varied for a given substance. Among native proteins a wide range of behavior for the tryptophan residues were found. The single tryptophan residues of HSA and RNase $T_1$ and the two residues of LADH were found to be held rigidly by the protein matrix. On the other hand, for myelin basic protein we found a highly mobile residue. We found that self-association of melittin resulted

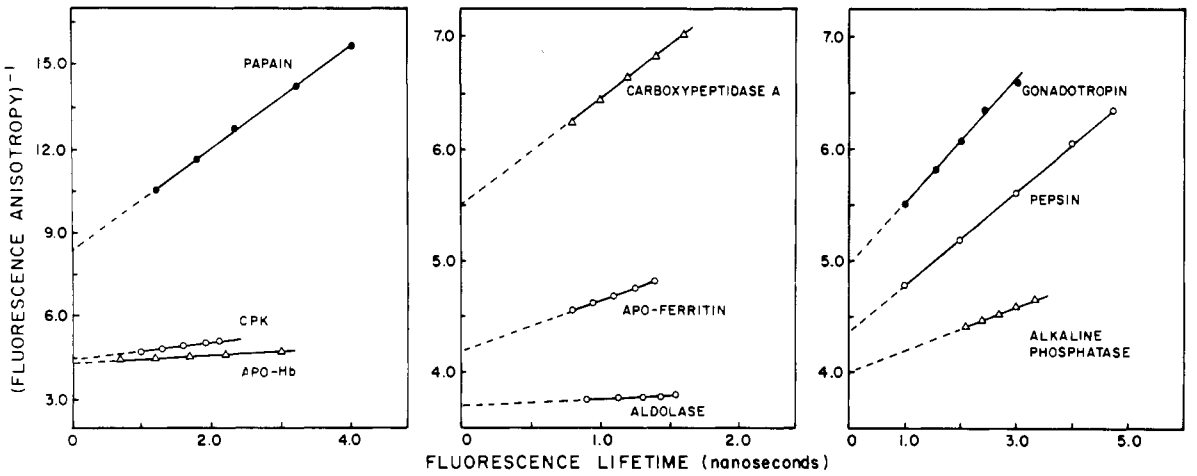


FIGURE 9: Lifetime-resolved anisotropies for multi-tryptophan proteins.

in an increase in the correlation time and that denaturation of HSA and monellin resulted in large decreases in their tryptophan correlation times. Hence it appears likely that the dynamic behavior of tryptophan residues in proteins is highly variable depending upon the protein and their localization within the folded protein matrix.

In addition, a number of multi-tryptophan proteins were studied. In these instances we could not assign correlation times to the individual residues. Instead we compared the average correlation time with that expected for a rigid hydrated sphere. For many proteins the observed correlation times were less than that calculated for the rigid sphere. Similar results were obtained earlier by Lakowicz & Weber (1980). In proteins containing several tryptophan residues one may expect that, on the average, some residues will be mobile and some rigidly by the protein matrix. For this reason measurement of the lifetime-resolved anisotropies of such proteins reveals, on the average, tryptophan residue mobility in excess of that expected for overall protein rotation.

It is interesting to compare the extent of tryptophan mobility revealed by our studies with the thermodynamic fluctuations predicted for molecules with a size comparable to that of a typical protein. For a protein with a molecular weight of 25 000 Cooper (1976) predicted that the root mean square fluctuation in energy to be 38 kcal/mol and the root mean square fluctuation in volume to be 30 cm$^3$/mol. The volume of an indole ring is about 100 cm$^3$/mol, as calculated from the radius of 3.4 Å given by Gladchenko & Pikulik (1967). Hence an angular displacement of this ring through an angle of about 30° would require a volume fluctuation comparable to that predicted by Cooper. Our data indicate that segmental motions of this magnitude are not unusual in proteins.

It is also interesting to compare our estimated correlation times and angular displacements with the predicted values of Karplus and co-workers (Karplus & McCammon, 1979). These workers estimated that the tyrosine residues of bovine pancreatic trypsin inhibitor will undergo angular displacements of 30° in 0.2 ps. A value of 30° is comparable to the larger values we found for the tryptophan residues. For all proteins we investigated the average displacement, in excess of overall protein rotation, was 17°, with a range from 0° to 37°. Recall that all our estimated values are minimal values, and the actual average angular freedom is likely to be larger. Recall also that our calculated angles are different from those reported by Karplus and co-workers, in that 54.7° is equivalent to complete depolarization. If our angles were expressed as angles within a cone, then the magnitudes would be larger and the average comparable to the 30° displacement calculated by Karplus and co-workers. Hence, the magnitude of the internal motions predicted by calculation and those determined experimentally seem to be comparable.

The agreement between the predicted correlation times for these motions seem less satisfactory. Admittedly, one should not compare the calculations on tyrosine residues with the measurements on tryptophan residues. If the tryptophan correlation times were as short as 0.2 ps, or even 2 ps, the effects of these rapid motions would be completed even at our shortest quenched lifetimes. These motions would not affect the apparent correlation times but would result in decreased values of $r(0)$. However, from Tables IV and V it is apparent that these apparent correlation times are shorter than expected, indicating that the time constants for a residue motion are at least 0.1 ns. Hence it appears either that the tryptophan residues undergo considerably slower motions than does tyrosine or that the molecular dynamic calculations overestimate the rates of structural fluctuations.

**Registry No.** NATA, 2382-79-8; Gly-Trp-Gly, 23067-32-5; Leu-Trp-Leu, 42293-99-2; Glu-Trp-Glu, 42293-97-0; Lys-Trp-Lys, 38579-27-0; alcohol dehydrogenase, 9031-72-5; RNase $T_1$, 9026-12-4; gastrin, 9002-76-0; cosyntropin, 16960-16-0; glucagon, 9007-92-5; melittin, 37231-28-0; micrococcal nuclease, 9013-53-0; chorionic gonadotropin, 9002-61-3; alkaline phosphatase, 9001-78-9; aldolase, 9024-52-6; creatine kinase, 9001-15-4; carboxypeptidase A, 11075-17-5; pepsin, 9001-75-6; papain, 9001-73-4; tryptophan, 73-22-3.

## References

Abdallah, M. A., Bielmann, J. F., Wiget, P., Jappich-Kuhn, R., & Luisi, P. C. (1978) *Eur. J. Biochem. 89*, 397–405.

Barboy, N., & Feitelson, J. (1978) *Biochemistry 17*, 4923–4926.

Bauer, D. R., Opella, S. J., Nelson, D. J., & Pecora, R. (1975) *J. Am. Chem. Soc. 97*, 2580–2582.

Belford, G. G., Belford, R. L., & Weber, G. (1972) *Proc. Natl. Acad. Sci. U.S.A. 69*, 1392–1393.

Bentz, J. P., Beyl, J. P., Beinert, G., & Weill, G. (1975) *Eur. Polym. J. 11*, 711–718.

Bernstein, R. S., Wilchek, M., & Edelhoch, H. (1969) *J. Biol. Chem. 244*, 4398–4405.

Bohak, Z., & Li, S. L. (1976) *Biochim. Biophys. Acta 427*, 153–170.

Brand, J. G., & Cagan, R. H. (1977) *Biochim. Biophys. Acta 493*, 178–187.

Bushueva, T. L., Busel, E. P., & Burstein, E. A. (1980) *Arch. Biochem. Biophys. 204*, 161–166.

Carerri, G. (1974) in *Quantum Statistical Mechanics in the Natural Sciences* (Kursunoglu, B., & Mintz, S. L., Eds.)

pp 15–35, Plenum Press, New York.
Carerri, G., Fasella, P., & Gratton, E. (1979) *Annu. Rev. Biophys. Bioeng. 8*, 69–97.
Chapman, B. E., & Moore, W. J. (1976) *Biochem. Biophys. Res. Commun. 73*, 758–766.
Chapman, B. E., & Moore, W. J. (1978) *Aust. J. Chem. 31*, 2367–2385.
Chen, R. F. (1973) *Arch. Biochem. Biophys. 158*, 605–622.
Cooper, A. (1976) *Proc. Natl. Acad. Sci. U.S.A. 73*, 2740–2741.
Eftink, M. R., & Ghiron, C. A. (1976) *Biochemistry 15*, 672–680.
Eftink, M. R., & Ghiron, C. A. (1977) *Biochemistry 16*, 5546–5551.
Eftink, M. P., & Jameson, D. M. (1982) *Biophys. J. 37*, 392a.
Eftink, M. R., & Selvidge, L. A. (1982) *Biochemistry 21*, 117–125.
Englander, S. W. (1975) *Ann. N.Y. Acad. Sci. 244*, 10–27.
Faucon, J. F., Dufourcq, J., & Lussan, C. (1979) *FEBS Lett. 102*, 187–190.
Feeney, J., Roberts, G. C. K., Brown, J. P., Burgen, A. S. V., & Gregory, H. (1972) *J. Chem. Soc., Chem. Commun.*, 601–604.
Georghiou, S., Thompson, M., & Mukhopadhyay, A. H. (1981) *Biochim. Biophys. Acta 642*, 429–432.
Gladchenko, L. F., & Pikulik, L. G. (1967) *J. Appl. Spectrosc. (Engl. Transl.) 6*, 355–360.
Gottlieb, Y. Y., & Wahl, P. (1963) *J. Chim. Phys. Phys.-Chim. Biol. 60*, 849–856.
Gurd, F. G., & Rothgeb, T. M. (1979) *Adv. Protein Chem. 33*, 73–165.
*Handbook of Biochemistry* (1970) 2nd ed., p J-279, CRC Press, Cleveland, OH.
Hanson, D. C., Yguerabide, J., & Schumaker, V. N. (1981) *Biochemistry 20*, 6842–6852.
Hilton, B. D., & Woodward, C. K. (1978) *Biochemistry 17*, 3325–3332.
Karplus, M., & McCammon, J. A. (1979) *Nature (London) 277*, 578.
Karplus, M., & McCammon, J. A. (1981) *CRC Crit. Rev. Biochem. 9*, 293–349.
Kawski, A., & Sepiol, J. (1972) *Bull. Acad. Pol. Sci., Ser. Sci., Math., Astron. Phys. 20*, 707–715.
Kinosita, K., Jr., Kawato, S., & Ikegami, A. (1977) *Biophys. J. 20*, 289–305.
Konev, S. V. (1967) *Fluorescence and Phosphorescence of Proteins and Nucleic Acids*, Plenum Press, New York.
Lakowicz, J. R. (1980) *J. Biochem. Biophys. Methods 2*, 91–119.
Lakowicz, J. R., & Weber, G. (1973a) *Biochemistry 12*, 4161–4170.
Lakowicz, J. R., & Weber, G. (1973b) *Biochemistry 12*, 4171–4179.
Lakowicz, J. R., & Knutson, J. R. (1980) *Biochemistry 19*, 905–911.
Lakowicz, J. R., & Weber, G. (1980) *Biophys. J. 32*, 591–601.
Lakowicz, J. R., Prendergast, F. G., & Hogen, D. (1979) *Biochemistry 18*, 520–527.
Lakowicz, J. R., Cherek, H., & Balter, A. (1981) *J. Biochem. Biophys. Methods 5*, 131–146.
Lipari, G., & Szabo, A. (1980) *Biophys. J. 30*, 489–506.
Liv, B. W., Cheung, H. C., & Mestecky, J. (1981) *Biochemistry 20*, 1997–2003.
Mantulin, W. W., & Weber, G. (1977) *J. Chem. Phys. 66*, 4092–4099.
Massey, J. B., & Churchich, J. E. (1979) *Biophys. Chem. 9*, 157–162.
McCammon, J. A., Gelin, B. R., & Karplus, M. (1977) *Nature (London) 267*, 585–590.
Munro, I., Pecht, K., & Stryer, L. (1979) *Proc. Natl. Acad. Sci. U.S.A. 76*, 55–60.
Nezlin, R. S., Zagyansky, Y. A., & Tumerman, L. A. (1970) *J. Mol. Biol. 50*, 569–572.
Purkey, R. M., & Galley, W. C. (1970) *Biochemistry 9*, 3569–3575.
Richards, F. M. (1974) *J. Mol. Biol. 82*, 1–14.
Richards, F. M. (1977) *Annu. Rev. Biophys. Bioeng. 6*, 151–176.
Ross, J. A. B., Chang, E. L., & Tiller, D. C. (1979) *Biophys. Chem. 10*, 217–220.
Ross, J. A. B., Rousslang, K. W., & Brand, L. (1981a) *Biochemistry 20*, 4361–4369.
Ross, J. A. B., Schmidt, C. J., & Brand, L. (1981b) *Biochemistry 20*, 4369–4377.
Saviotti, M. L., & Galley, W. C. (1974) *Proc. Natl. Acad. Sci. U.S.A. 71*, 4154–4158.
Spencer, R. D., & Weber, G. (1969) *Ann. N.Y. Acad. Sci. 158*, 361–376.
Spencer, R. D., & Weber, G. (1970) *J. Chem. Phys. 52*, 1654–1663.
Steiner, R. F. (1971) *Biochemistry 10*, 771–778.
Talbot, J. C., Dufourcq, J., de Bony, J., Faucon, J. F., & Lussan, C. (1979) *FEBS Lett. 102*, 191–193.
Teale, F. W. J., & Badley, R. A. (1970) *Biochem. J. 116*, 341–348.
Vanderkooi, J. M., Calhoun, D. B., & Englander, S. W. (1982) *Biophys. J. 37*, 248a.
Wagner, G., & Wuthrich, K. (1978) *Nature (London) 275*, 247–248.
Wahl, Ph., & Weber, G. (1967) *J. Mol. Biol. 30*, 371–382.
Wallach, D. (1967) *J. Chem. Phys. 47*, 5258–5268.
Weber, G. (1952) *Biochem. J. 51*, 145–155.
Weber, G. (1960) *Biochem. J. 75*, 335–345.
Yguerabide, J., Epstein, H. F., & Stryer, L. (1970) *J. Mol. Biol. 51*, 573–590.